## 3.2.4 The phylogeny of *Lasioserica*

### Material and methods

*Taxon sampling and characters*

Sixty-one species belonging to three genera were examined for the cladistic analysis. Character coding was based on 59 species and subspecies so far assigned to *Amiserica* Nomura, 1974 and *Lasioserica* Brenske, 1896 (see appendix A 3.2.4). Additionally, *Maladera holosericea* was included in the analysis. Due to the still completely unexplored generic relationships, *Pleophylla* sp. was chosen as an outgroup taxon being with high probability not part of the ingroup (chapter 3.1). The choice of the taxa included into ingroup was mainly based on present and historical classification of the species and genera of the genus *Lasioserica* (e.g. Brenske 1898; Nomura 1974; Ahrens 2000e; Yu et al. 1998) based on the original diagnosis of the original description of *Lasioserica* (Brenske 1896). Eighty-six adult characters were scored here. The character states are illustrated in Figs 57-62.

*Phylogenetic analysis*

The 84 characters (54 binary and 30 multistate) were all unordered and equally weighted. Inapplicable characters were coded as "-", while missing character states were coded as "?" (Strong and Lipscomb 1999). Uninformative characters were excluded from analysis when they were identified as apomorphies of a terminal taxon. The parsimony analysis was performed in NONA 2.0 (Goloboff 1999) using the parsimony ratchet (Nixon 1999) implemented in NONA, run with WINCLADA vs. 1.0.08 (Nixon 2002) as a shell program. Two hundred iterations were performed (one tree hold per iteration). The number of characters to be sampled for reweighting during the parsimony ratchet was determined to be eight. All searches were done under the collapsing option "ambiguous" which collapses every node with a minimum length of 0. State transformations were considered to be apomorphies of a given node only if they were unambiguous (i.e., without arbitrary selection of accelerated or delayed optimization) and if they were shared by all dichotomised most parsimonious trees. Bremer support (Bremer 1988, 1994) and parsimony jackknife percentages (Farris et al. 1996) were evaluated using NONA. The search was set to a Bremer support level of 12, with seven runs (each holding a number of trees from 100 to 500 times multiple of suboptimal tree length augmentation) and a total hold of 8000 trees. The jackknife values were calculated using 100 replications and a 100 search steps (mult*N) having one starting tree per replication (random seed 0). Character changes were mapped on the consensus tree using WINCLADA.

Successive approximations weighting (Farris 1969) was used to further evaluate phylogenetic relationships. This method uses *post hoc* character weighting based on the fit of each character as applied to the trees currently in memory. Thus, the 'quality' of the character data is used rather than intuitive feeling regarding weighting of characters. Although this method increases the assumptions in the analysis (Siebert 1992), it is useful for hypothesizing phylogenetic pattern when characters exhibit a high level of homoplasy, and it is recursive (Wenzel 2001) and not circular, as for example Wägele (2000) stated, because it yields different sets of trees in subsequent iterations. Characters were reweighted based on the rescaled consistency index and on the consistency index. The base weight was set at 100 and weights were manually inserted in parsimony ratchet of NONA via the WINCLADA user surface. Tree searches continued until the character weights no longer changed (Farris 1988) which in the present search were respectively three iterations for consistency index based successive weighting, and four iterations rescaled consistency index based successive weighting.

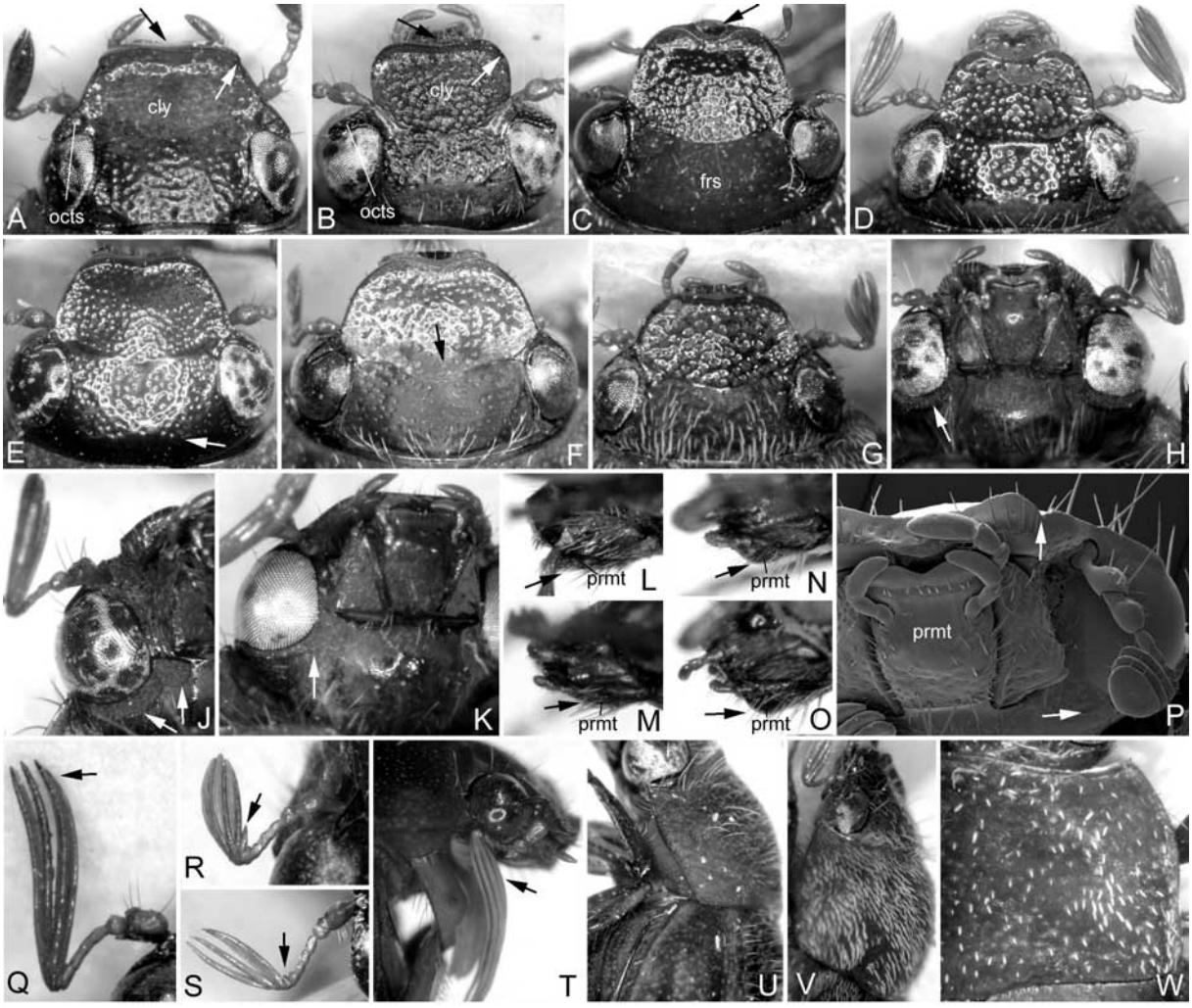


**Fig. 57. A:** *Amiserica patibilis*; **B:** *Lasioserica dragon*; **C, S:** *L. pudens*; **D, H, O:** *L. modikholae*; **E:** *L. nobilis*; **F, R:** *L. assamicola*; **G, V:** *L. turaensis*; **J, N, U:** *L. maculata jiriana*; **K:** *A. chiangdaoensis*; **L:** *Pleophylla* sp.; **M, P:** *A. krausei*; **Q:** *L. brevipilosa*; **T:** *A. antennalis*; **W:** *L. dekensis.* **A-G:** head, dorsal view; **H-K, P:** head, ventral view; **L-O:** labium, lateral view; **Q-T:** antenna; **U,V:** head and pronotum, lateral view; **W:** pronotum, dorsal view (not to scale).

## Characters and character states

In describing character states, I refrained from formulating any hypothesis about their transformation. In particular, coding does not imply whether a state is derived or ancestral. The data matrix, and in addition to the character description, consistency index (ci) and retention index (ri) calculated by WINCLADA analysis are given in appendix B 3.2.4.

*Head*

1. *Labroclypeus, surface*: (0) completely shiny (Figs 57A-E,G); (1) basally dull (Fig. 57F).
2. *Labroclypeus, anterior margin*: (0) reflexed as strongly as lateral margins (Figs 57B-G); (1) more strongly reflexed than lateral margins (Fig. 57A, black arrow).
3. *Labroclypeus, anterior angles*: (0) strongly rounded (Figs 57B-G); (1) weakly rounded (Fig. 57A).
4. *Labroclypeus, lateral margin*: (0) not incised (Figs 57B, white arrow, C-G); (1) incised preapically (Fig. 57A, white arrow).
5. *Labroclypeus, anterior margin medially*: (0) distinctly sinuate (Figs 57C, black arrow, D); (1) weakly sinuate (Figs 57B,E,G); (2) not sinuate (Fig. 57A).
6. *Frons*: (0) completely dull (Figs 57C,F,G); (1) posteriorly dull only (Figs 57B,D); (2)

completely shiny (Figs 57A,E).

7. *Frons, pilosity*: (0) present (Figs 57B-D,F,G); (1) absent (Figs 57A,E).
8. Lateral margin of labroclypeus and ocular canthus produce: (0) a distinct and blunt angle (Figs 57A,G); (1) an indistinct angle (Figs 57B-F).
9. *Postocular furrow*: (0) not reaching the interior margin of the eye (Fig. 57K); (1) protruding medially the interior margin of the eye (Figs 57H,J).
10. *Prementum distally*: (0) moderately convex (less high than half of maximal width of labium) (Fig. 57N); (1) flattened (Figs 57L,M); (2) strongly convex (approximately as high as half of maximal width of labium) (Fig. 57O).

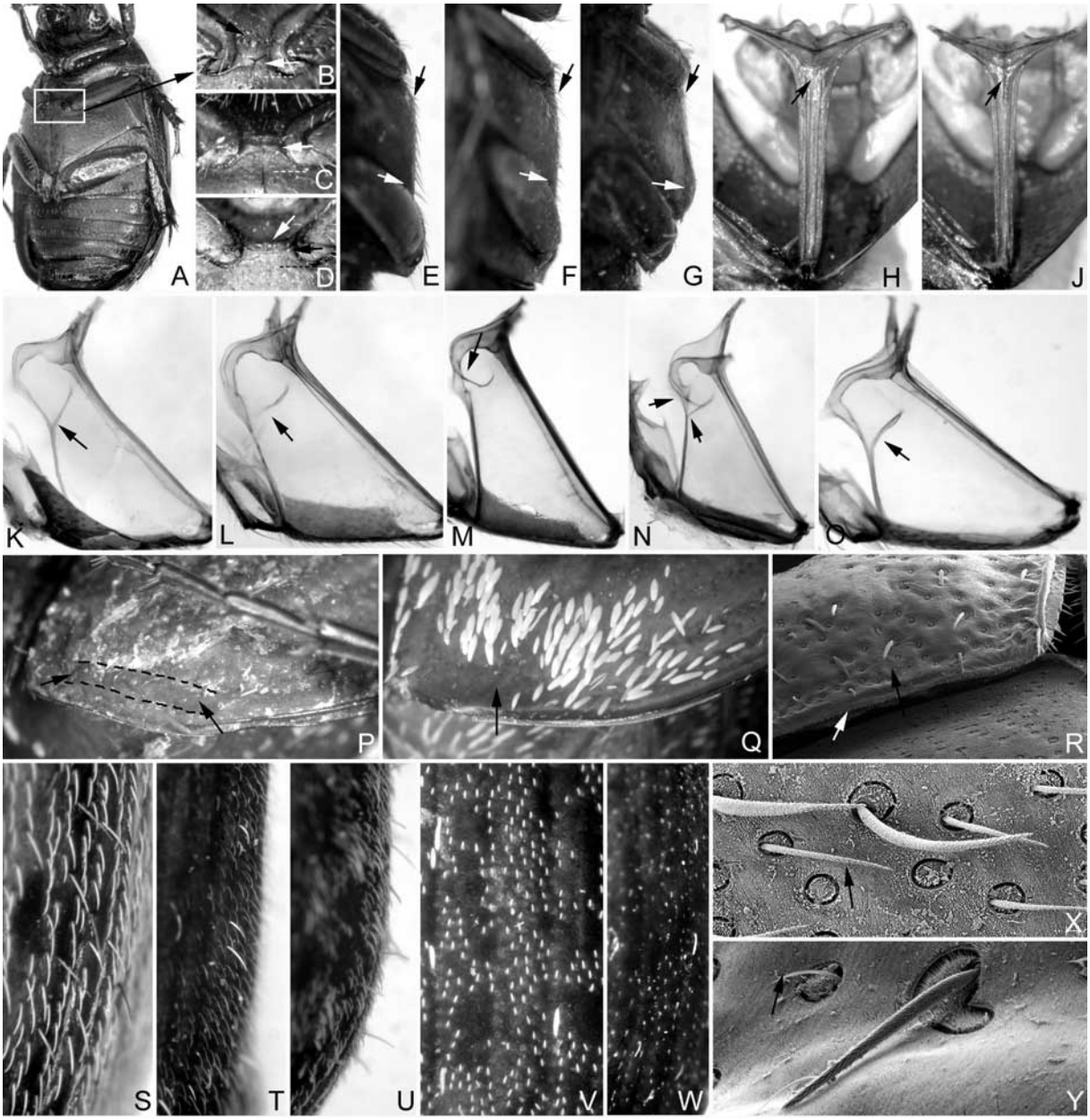


**Fig. 58. A:** *Lasioserica modikholae*; **B:** *Amiserica patibilis*; **C:** *L. tenera*; **D, F, H:** *A. chiangdaoensis*; **E:** *L. sabatinellii*; **G, J, O, R:** *A. krausei*; **K, P:** *L. nobilis*; **L:** *L. chitreana*; **M:** *A. flavolucida*; **N:** *L. meghalayana*; **Q:** *L. pudens*; **S:** *Pleophylla* sp.; **T, X:** *L. brevipilosa*; **U:** *L. turaensis*; **V:** *L. immatura*; **W, Y:** *L. modikholae.* **A:** body lateroventral view;-**B-D:** meso- and metasternum between mesocoxae, ventral view; **E-G:** metasternum, lateral view; **H, J:** metafurca, dorsal view; **K-O:** metafurca, lateral view; **P-R:** apex of elytra, dorsoapical view; **S-U:** detail of elytra, lateral view; **V, W:** detail of elytra, dorsal view; **X, Y:** setae and punctation of elytra (SEM) (not to scale).

11. *Labrum medially*: (0) weakly sinuate (Figs 57A,B, black arrow, E,G); (1) strongly sinuate (Figs 57C, black arrow, D,F).
12. *Number of antennomeres*: (0) ten (Figs 57Q-T); (1) nine (Fig. 57P); (2) nine or ten.
13. *Antennal club*: (0) as long as remaining antennomeres combined (Fig. 57S); (1) 1.5 times as long as remaining antennomeres combined; (2) twice as long as remaining antennomeres combined (Figs 57Q,T); (3) shorter than the remaining antennomeres combined (Figs 57P,R).
14. *Antennomere seven*: (0) not transversely produced (Fig. 57S); (1) transversely produced, at maximum one third of length of antennal club (Fig. 57R); (2) transversely produced, at least half of length of antennal club (Figs 57D,G,Q,T).

*Thorax*

15. *Body, pilosity of dorsal surface*: (0) double (Figs 58S-Y); (1) simple (Fig. 57U).
16. *Pilosity on pronotum and elytra*: (0) adpressed or directed posteriorly (Figs 57V,W, 58S-W); (1) erect (Fig. 57U).
17. *Pilosity of pronotum*: (0) fine (Fig. 57U); (1) with robust scales (Figs 57V,W); (2) very minute or reduced (Fig. 57T).
18. *Pronotum, anterior margin*: (0) complete; (1) narrowly interrupted medially; (2) widely interrupted medially.
19. *Metasternum mesoposteriorly*: (0) not elevated in contrast to anterior portion (Fig. 58G); (1) strongly elevated in contrast to anterior portion (Figs 58E,F).
20. *Metasternum in anterior half*: (0) convex (Fig. 58E); (1) flat or concave (Figs 58F,G).
21. *Metasternum, anterior margin medially*: (0) weakly produced (Fig. 58B); (1) strongly produced (Figs 58C,D).
22. *Metafurca, median keel dorsoposteriorly*: (0) almost complete from base to apex; (1) present only in distal portion (circa 1/5 or less) (Fig. 58J); (2) completely absent (Fig. 58H).
23. *Metafurca, lateral lamina anteriorly*: (0) curved dorsally (Fig. 58M); (1) almost straight, directed ventrally (Figs 58K,L,O); (2) duplicate, one curved dorsally, one straight directed ventrally (Fig. 58N).
24. *Metafurca, relation of maximal width of metafurcal arms/ length anterior edge- caudal apex of metafurcal arms*: (0) large (Fig. 60C); (1) small (Fig. 60D).
25. *Elytra, fine pilosity*: (0) fine (Figs 58S,T,X); (1) reduced (minute only) (Figs 58W,Y); (2) thickened (Fig. 58U); (3) scale like (Figs 58Q,V).
26. *Elytra, microtrichomes on apical margin*: (0) present (Figs 58P-R, white arrow); (1) absent.
27. *Elytra, epipleural edge*: (0) simple, not elevated apically (Figs 58Q, black arrow, R); (1) strongly elevated apically (Fig. 58P, black arrow).

*Legs*

28. *Metafemur, posterior margin ventrally*: (0) not serrate (Figs 59A,P); (1) finely serrate; (2) strongly serrate.
29. *Legs, metafemur, posterior margin dorsally*: (0) smooth; (1) serrate (Fig. 59F).
30. *Metafemur, posterior margin ventrally*: (0) sharply edged in distal half (Figs 59A-D,F); (1) sharply edged in distal three quarter of femoral length (Fig. 59E).
31. *Metafemur, submarginal serrated line*: (0) absent (Figs 59A,B); (1) present (Figs 59C-F).
32. *Metafemur, submarginal serrated line*: (0) entirely separated from anterior margin (Fig. 59D); (1) not entirely separated from anterior margin (Figs 59C,E).
33. *Metafemur, pilosity ventrally*: (0) immediately behind submarginal serrated line (Figs 59C,E); (1) with a small distance to submarginal serrated line (Fig. 59D).

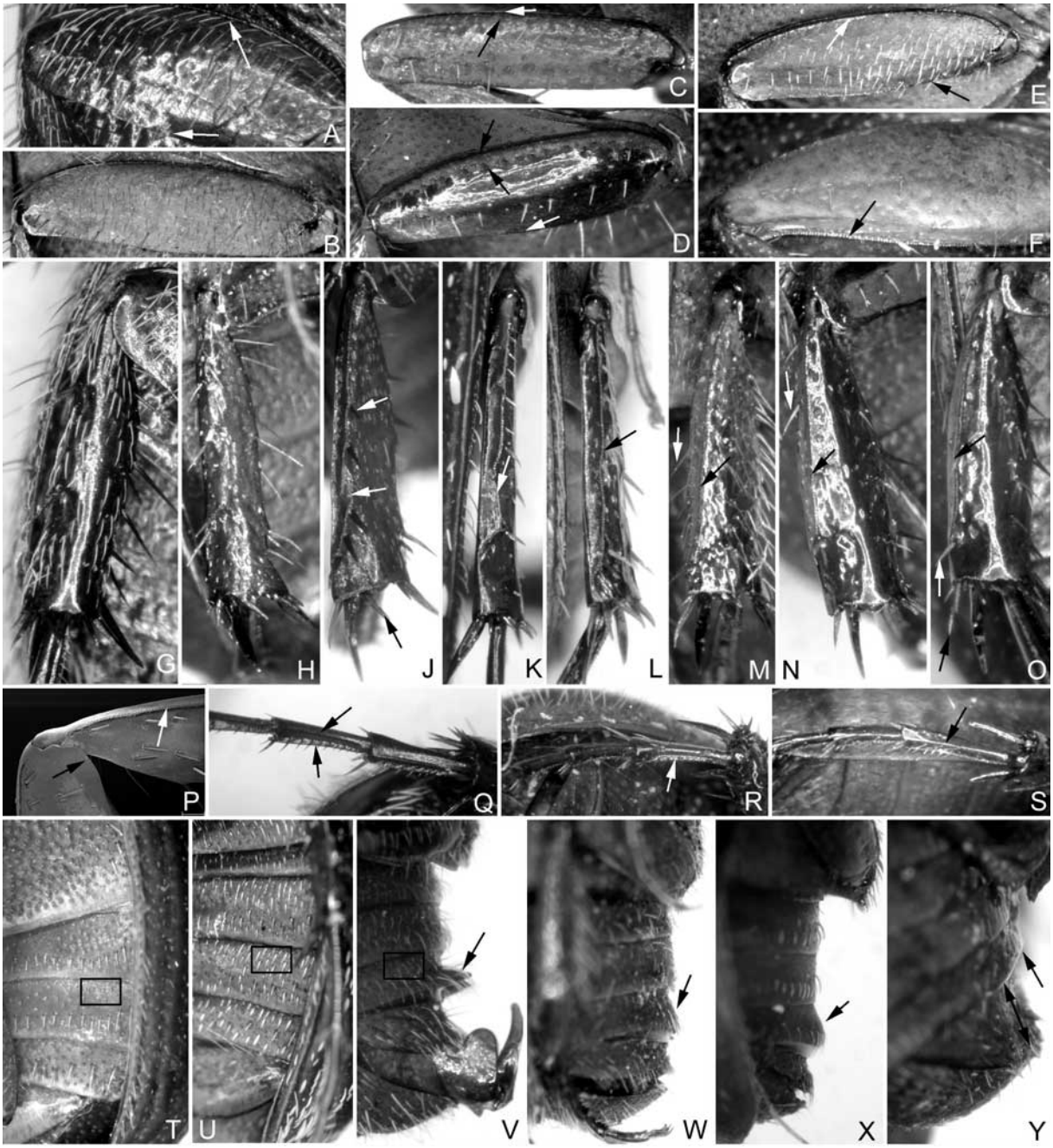


**Fig. 59. A, G, Q:** *Pleophylla* sp.; **B:** *Calloserica langtangica*; **C:** *Amiserica antennalis*; **D, O, P, X:** *Lasioserica modikholae*; **E:** *A. chiangdaoensis*, **F:** *L. assamicola*; **H:** *L. dragon*; **J:** *A. rufidula*; **K, U:** *L. pudens*; **L:** *L. dekensis*; **M, R, W:** *L. maculata jiriana*; **N:** *L. meghalayana*; **S:** *L. brevipilosa*; **T:** *A. antennalis*; **V:** *L. tenera*; **Y:** *A. krausei*. **A-F:** metafemur, ventral view; **G, H, N, O:** metatibia, lateral view; **J-M:** metatibia, dorsolateral view; **P:** metafemur, ventrolateral view; **Q-S:** basal metatarsomeres, lateral view; **T-Y:** abdomen, lateral view (not to scale).

34. *Mesotibia, apical spine*: (0) straight (Fig. 60E); (1) curved ventrally at apex (Fig. 60G); (2) curved ventrally at middle (Fig. 60F).
35. *Metatibia, longitudinally serrated keel beside dorsal margin*: (0) absent (Figs 59G,H); (1) present (Figs 59J-O, black arrow).
36. *Metatibia, longitudinally serrated keel beside dorsal margin*: (0) straight (Figs 59L-O); (1) undulate.
37. *Metatibia, longitudinal serrated keel beside dorsal margin*: (0) not interrupted (Figs 59L-O); (1) not constantly uninterrupted, often interrupted once in distal half (Figs 59J,K, white arrow); (2) always interrupted several times along overall length.

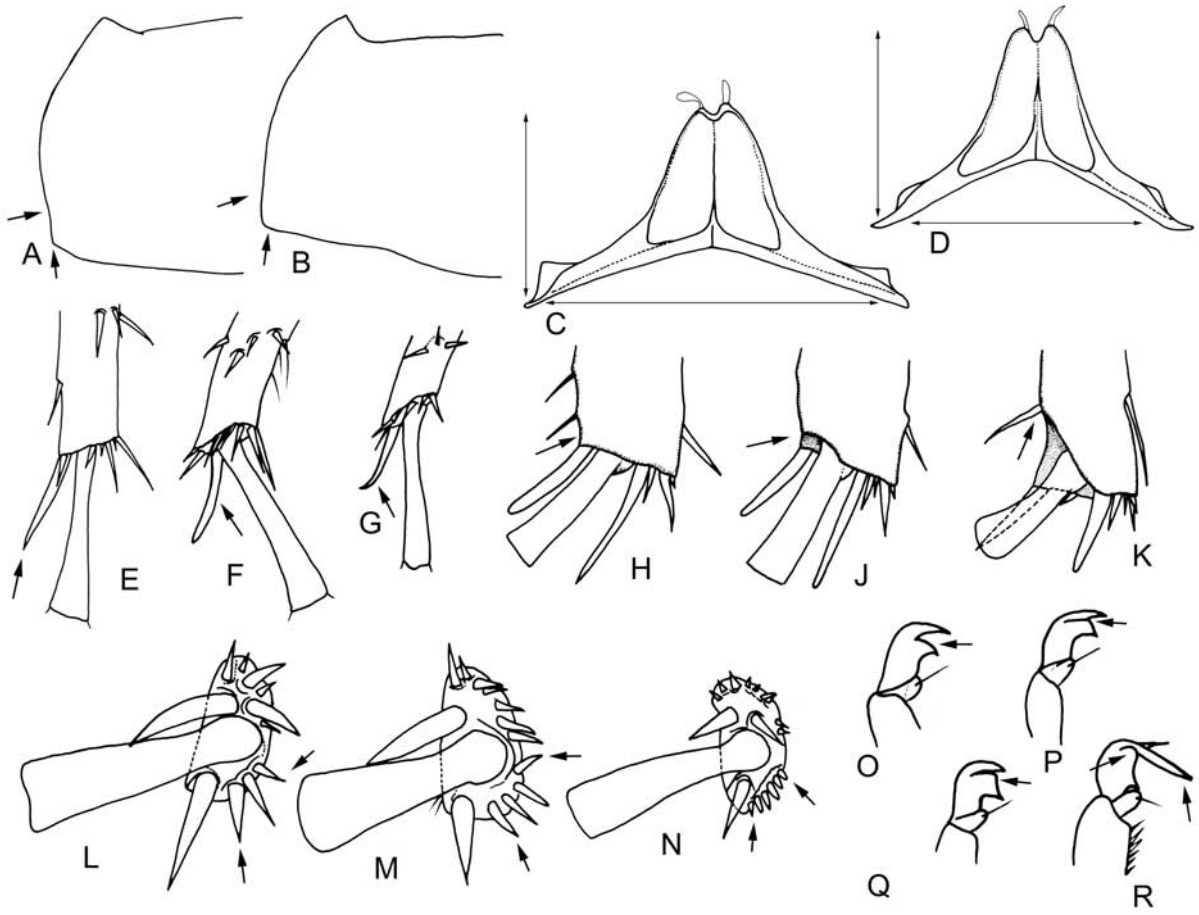


**Fig. 60. A:** *Amiserica krausei*; **B:** *Lasioserica assamicola*; **C:** *L. maculata maculata*; **D:** *L. brevipilosa*; **E:** *Pleophylla* sp.; **F, J, M, O:** *L. nepalensis*; **G:** *L. tenera*; **H, L, Q:** *A. rufidula*; **K, N, P:** *A. krausei*; **R:** *A. patibilis*. **A, B:** pronotum, left half in dorsal view; **C, D:** metafurca, craniodorsal view; **E-G:** apex of mesotibia, lateral view; **H-K:** apex of metatibia, medial view; **L-N:** apex of metatibia, apical view; **O, P, R:** internal protarsal claw; **Q:** external protarsal claw (not to scale).

38. *Metatibia, apical margin on medial face*: (0) weakly concavely sinuate, forming a distinct angle with ventral margin (Fig. 60J); (1) obtusely moderately truncate, forming an indistinct angle with ventral margin (Fig. 60H); (2) deeply and acutely truncate (Fig. 60K).
39. *Metatibia, dorsal margin*: (0) acutely edged (Figs 59J-L); (1) moderately edged (Figs 59M,N); (2) longitudinal convex (Figs 59A,O).
40. *Metatibia, between longitudinal keel and dorsal margin*: (0) punctate and with numerous setae (Fig. 59M); (1) punctate and glabrous (Fig. 59L); (2) smooth (Fig. 59O) (3) punctate and with one robust seta only behind basal third (Fig. 59N).
41. *Metatibia, spines along dorsolateral longitudinal carina*: (0) as robust as apical spines (Figs 59J-L); (1) only basal spines finer than apical spines (Fig. 59N); (2) all spines finer than apical spines (Figs 59M,O).
42. *Metatibia, number of ventral spines on apical face*: (0) four (Fig. 60M); (1) three (Fig. 60L); (2) five; (3) six (Fig. 60N).
43. *Metatibia, interior spines on apical face*: (0) absent (Figs 60L,M); (1) present (Fig. 60N).
44. *Interior protarsal claw, basal tooth*: (0) normally pointed at the tip (Fig. 60O); (1) truncate at the tip (Fig. 60P); (2) 0&1; (3) lobiform (Fig. 60R).
45. *External protarsal claw, basal tooth*: (0) normally pointed at the tip; (1) truncate at the tip (Fig. 60Q); (2) lobiform.
46. *Mesotarsomeres, ventral median carina*: (0) present; (1) absent.

47. *Mesotarsomeres, supplementary ventrolateral carina*: (0) present; (1) absent.
48. *Metatarsomeres laterally*: (0) without lateral carina (Figs 59Q,R); (1) with lateral carina (Fig. 59S).
49. *Metatarsomeres, supplementary subventral carina beside serrated ventral carina*: (0) present (Fig. 59Q); (1) absent (Figs 59R,S).
50. *Metatarsomeres dorsally*: (0) punctate (Fig. 59S); (1) impunctate (Figs 59Q,R).

*Abdomen*

51. *Diffuse fine setae of abdominal sternites (not those setae of transverse rows of coarse punctures)*: (0) long (Figs 59U,V (black frame), W); (1) absent or minute (distinctly shorter than those of transverse rows of coarse punctures) (Figs 59T (black frame), X).
52. *Last abdominal sternite*: (0) as long or shorter than the penultimate sternite (Figs 59V-X, 61B,C); (1) distinctly longer than the penultimate sternite (Figs 59Y, 61A).
53. *Last abdominal sternite, mesoposteriorly (ventral view)*: (0) not concavely sinuate (Fig. 61A); (1) weakly (by ¼ of length of sternite) concavely sinuate (Figs 61B,C); (2) strongly (by more than half of length of sternite) concavely sinuate.
54. *Penultimate abdominal sternite*: (0) without two tubercles (Figs 59X,Y, 61A,B); (1) with two tubercles (Figs 59V, 61C).

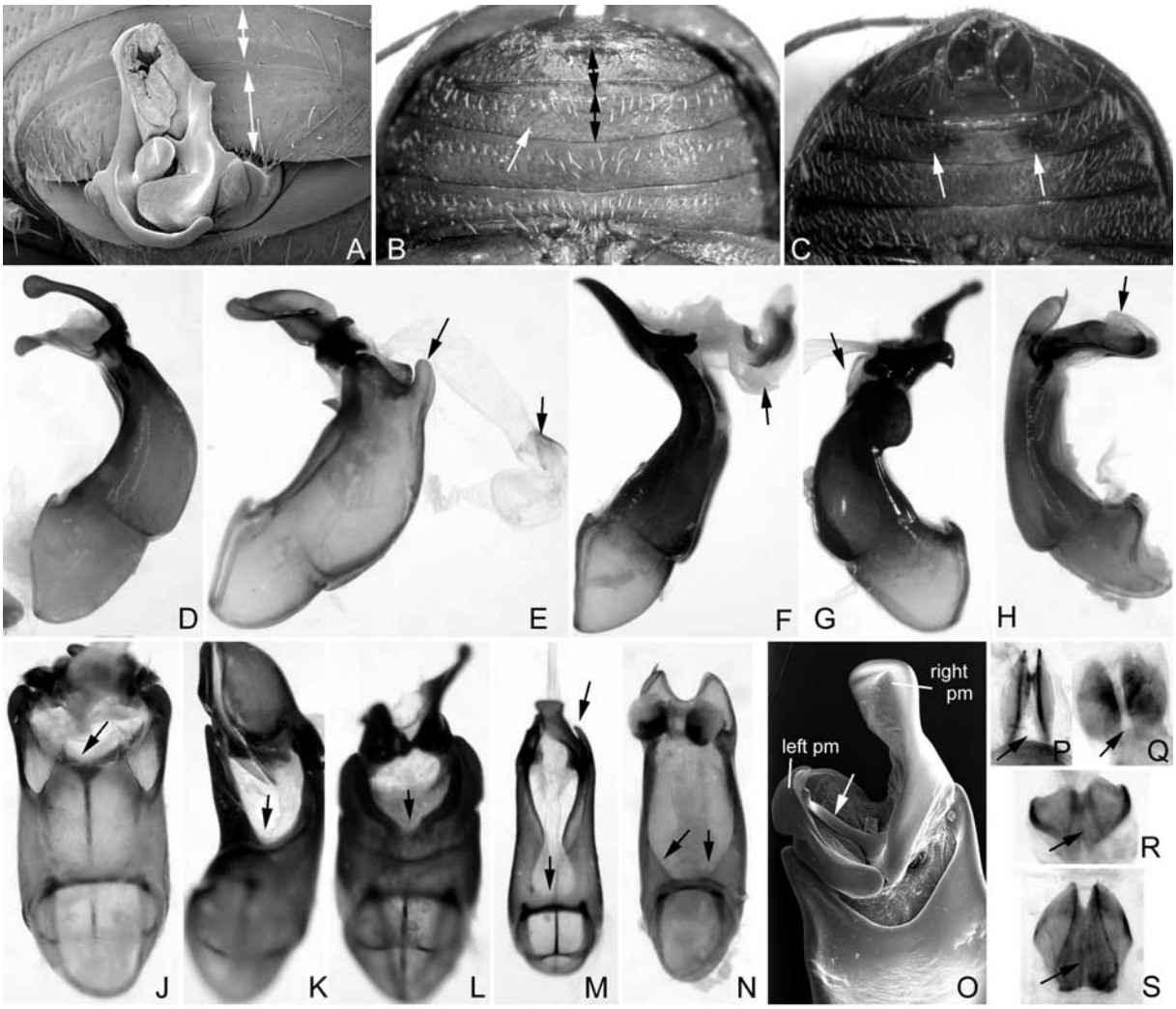


**Fig. 61. A:** *Amiserica krausei*; **B:** *Lasioserica meghalayana*; **C:** *L. tenera*; **D:** *L. pudens*; **E, R:** *L. maculata maculata*; **F, K, Q:** *A. chiangdaoensis*; **G, L:** *L. brevipilosa*; **H, N:** *A. rufidula*; **J, P:** *A. krausei*; **M:** *L. chitreana*; **O:** *L. modikholae*; **S:** *L. pacholatkoi*. **A-C:** abdomen, ventral view; **D-F:** aedeagus, right side lateral view; **G, H:** aedeagus, left side lateral view; **J-O:** aedeagus, ventral view; **P-S:** temones, dorsal view (not to scale).

55. *Tubercles on penultimate abdominal sternite*: (0) small and convex; (1) large and acute (Figs 59V, 61C).
56. *Penultimate abdominal sternite*: (0) flat (Figs 59W,Y); (1) transversely elevated (Fig. 59X).
57. *Pygidium in female*: (0) simply convex; (1) in basal half with median keel.

*Male genitalia*

58. *Phallobase ventroapically*: (0) weakly sinuate (Figs 61L,O); (1) moderately narrowly incised; (2) deeply narrowly incised (Fig. 61M); (3) widely deeply incised (Figs 61K,N); (4) within median sinuation medially convexly produced apically (Fig. 61J).
59. *Phallobase at apex (dorsal view)*: (0) not widened, slightly narrower than in the middle (Figs 62A,B,E,T-V); (1) widened, as wide or wider as in the middle (Figs 62C, 61J,O).
60. *Phallobase in apical half (dorsal view)*: (0) not or weakly narrowed (Figs 62A-D,T-V) (1) strongly narrowed (Figs 62E, arrow, Bb).
61. *Phallobase mesoapically (dorsal view)*: (0) simply sinuate (Figs 62A-E,Y-Aa, Cc,Dd,Ff); (1) within sinuation with a triangular median process (Fig. 62F).
62. *Phallobase apically at left side*: (0) not produced and the insertion of parameres not protruding (Figs 62A-F,K,M,N,T-W,Y-Ff); (1) produced and the insertion of parameres protruding (Figs 62J,L,R,S); (2) 0&1.
63. *Phallobase apically at right side*: (0) not produced protruding the insertion of parameres (Figs 62A-F,O,P,R-V,X-Cc,Ee,Ff); (1) produced protruding the insertion of parameres (Figs 62Q,Dd).
64. *Phallobase lateroventrally*: (0) not lamellously produced and elevate (Figs 62H,J,Q,W,X); (1) at middle lamellously produced and elevate (Figs 62M,N); (2) at apex lamellously produced and elevate (Figs 62F,G,K,Aa).
65. *Phallobase ventrally, median sinuation*: (0) without median sclerotized trunk (Figs 61J-O, 62S-V,Bb,Ee); (1) with median sclerotized trunk (Fig. 62R).
66. *Phallobase ventromedially*: (0) without median longitudinal excavation (Figs 61K,M,N); (1) with distinctly pronounced median longitudinal excavation (Figs 61J,L).
67. *Phallobase ventrally, before apical third*: (0) without transverse tubercles (Figs 62R,S); (1) with two small transverse tubercles (Figs 62G,V); (2) with two lobiform transverse carinae (Figs 62T,U).
68. *Phallobase, distal portion of apical longitudinal elevations*: (0) without microraster; (1) with microraster (90X magnification) (Fig. 62Aa).
69. *Phallobase dorsally, basally of median apical sinuation*: (0) simple, without any apophysis (Figs 61D,F-H, 62A-C,F,H,K-O,Q,Y-Aa,Cc,Dd,Ff); (1) with apophysis round in cross-section (Figs 61E, 62D,J,P,S,W,X).
70. *Aedeagus, medioapical dorsal apophysis*: (0) long (longer than parameres) (Fig. 62W); (1) short (as long or shorter than parameres) (Figs 61E, 62D,J,P,S,X).
71. *Phallobase, dorsal apophysis distally*: (0) convex; (1) sinuate medially.
72. *Phallobase laterally at left side*: (0) without dorsally produced lobe (Figs 62H-N); (1) with dorsally produced lobe before insertion of parameres (Fig. 62W).
73. *Parameres*: (0) equal in length (Figs 61H, 62A,Cc,Ff); (1) left paramere little shorter than the right (Figs 62B,F,M); (2) left paramere half as long as the right (Figs 61G, 62N,Z); (3) left paramere less than one third as long as the right.
74. *Parameres*: (0) almost symmetrical (Fig. 62Ff); (1) asymmetrical (Figs 62A-Ee).
75. Parameres, at apex: (0) without membraneous sacks (Figs 61D-G); (1) with membraneous sacks (Fig. 61H, arrow).
76. *Parameres basiventrally*: (0) separate (Figs 61K-O); (1) fused (Fig. 62Bb).

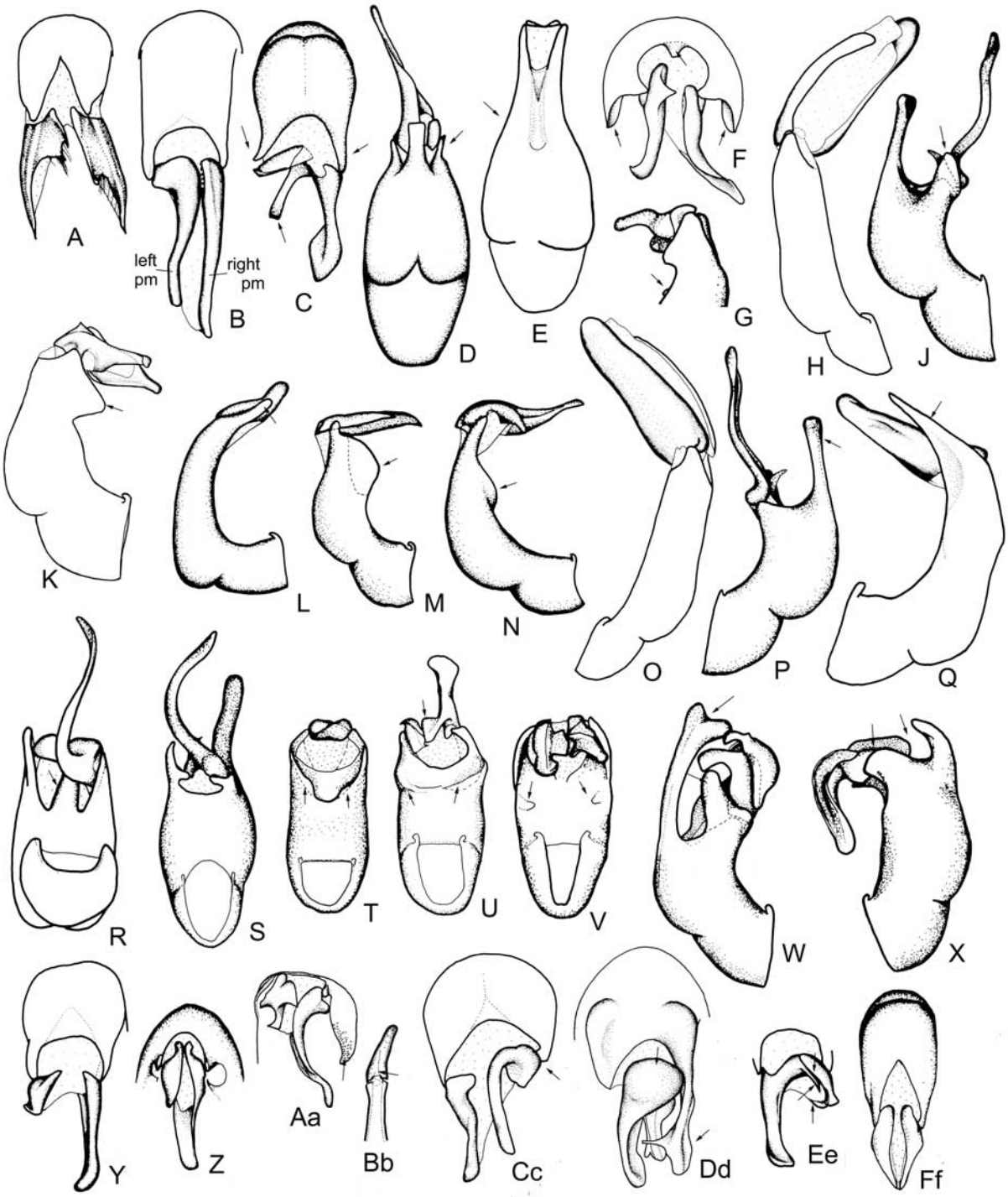


**Fig. 62. A:** *Pleophylla* sp.; **B, H, O:** *Lasioserica assamicola*; **C:** *L. godavariensis*; **D:** *L.bumthangana*, **E:** *L. soror*; **F, K:** *L. itohi*; **G, V:** *L. brevipilosa*; **J, P, S:** *L. silkae*; **L:** *L. chitreana*, **M, T:** *L. pilosella*; **N, Z:** *L. piloselloida*; **Q:** *L. orlovi*; **R:** *L. nenya*; **U:** *L. nepalensis*; **W:** *L. nobilis*; **X:** *L. maculata maculata*; **Y, Ee:** *L. dolakhana*; **Aa:** *L. tricuspis*; **Bb:** *L. thoracica*; **Cc:** *L. pudens*; **Dd:** *L. pacholatkoi*; **Ff:** *A. manipurensis.* **A-C, F, Y-Aa, Cc, Dd, Ff:** parameres, dorsal view; **D, E:** aedeagus, dorsal view; **G:** parameres, right side lateral view; **H-N, W:** aedeagus, left side lateral view; **Q, X:** aedeagus, right side lateral view; **R-V:** aedeagus, ventral view; **Bb, Ee:** parameres, ventral view (not to scale).

77. *Right paramere*: (0) straight (Figs 62A-C,F,Y,Aa,CC,Ff); (1) medial face rotated 90° to dorsal face (Figs 62P,Z); (2) medial face rotated 180° to external face (Fig. 62X).
78. *Right paramere inserted at phallobase*: (0) at same level as the left one (Figs 62A-F,Y,Z,Ff); (1) displaced distally (Fig. 62X); (2) displaced basally (Fig. 62Cc).
79. *Right paramere basomedially*: (0) simple (Figs 61K-N); (1) with a large blunt tooth (Fig.

62U); (2) with a long and sharply produced branch (Figs 61O, 62C,Ee).
80. Left paramere, apically: (0) straight (Figs 61G, 62H,K-N); (1) curved dorsally (Fig. 62W).
81. *Left paramere in cross section*: (0) simple, weakly arched; (1) strongly arched, medial face longitudinally concave, external face longitudinally convex (Figs 61O, 62Ee).
82. Left paramere, basally: (0) without lobe; (1) with short and spherical lobe.
83. *Endophallus*: (0) without dorsal lobe (Figs 61D,E,H); (1) with double dorsal lobe before base of parameres (Fig. 61F); (2) with single dorsal lobe before base of parameres (Fig. 61G).
84. *Endophallus, temones*: (0) separate (Figs 61P,Q); (1) basal portion mesally fused (Figs 61R,S); (2) entirely fused mesally.

From former original data set two characters have been omitted from analysis: (A) pronotum, lateral margins in posterior half: (0) not convergent posteriorly (Figs 57W, 60B); (1) convergent posteriorly (Fig. 60A); (2) 0&1; (B) mesosternum, setae between mesocoxae: (0) unevenly distributed (Fig. 58B); (1) on a semicircular anteriorly opened edge (Figs 58C,D); (2) 0&1. Due to their polymorphic states and also high intraspecific variability within a presumptive lineage they caused a high degree of polytomy in the strict consensus tree and hence a strongly ambiguous and 'noisy' phylogenetic signal. However, due to the very limited number of specimens of some taxa available for study, this variability could not be assessed. Nevertheless, they were noticed here, since they are notwithstanding their variability of diagnostic importance, and at least the latter character seems to me to be worthy of investigation in a wider context of phylogeny of sericine genera.

## Results

The analysis of 84 adult characters with the parsimony ratchet using the above mentioned settings yielded 330 equally parsimonious trees of 344 steps (CI: 0.37, RI: 0.72). The strict consensus of these trees, with jackknife values and Bremer support, is presented in Fig. 63 as the preliminary hypothesis of relationships between the taxa showing areas of tree conflict as polytomies. Repeating the parsimony ratchet with modified settings (1000 iterations and ten trees hold per iteration with ten sequential ratchet runs) resulted not in a shorter tree or a modified topology of the strict consensus tree but in an increasing number of equally parsimonious trees. The tree topology was not affected by altering ACCTRAN or DELTRAN optimization.

The strict consensus (Fig. 63) shows in some parts polytomy which must attributed to a high degree of homoplasy among characters included in the analysis. On the other hand, in several cases, such as for the *Lasioserica nepalensis*-group, or the *L. brevipilosa*-group, I refrained from including further characters helping to resolve the tree topology, since these characters with high probability would have augmented homoplasy in the data matrix. To assume in some manner information of the high number of equally parsimonious trees resulted from the parsimony ratchet with equally weighted characters, a majority rule consensus tree was generated (Fig. 64).

To further examine phylogenetic pattern and to reduce the number of equally parsimonious trees, I used successive approximations character weighting (SACW, Farris 1969) applying a weighting scheme based on the consistency index and the rescaled consistency index. Most parsimonious trees (MPTs) yielded by SACW are as long (344 steps in the ci based and in the rc based SACW scheme) as MPTs resulting from the original data set. In both analyses, use of successive approximations character weighting (SACW) greatly improved strict consensus tree resolution resulting in tree topologies found also in the original set of equally weighted

most parsimonious trees as indicated by tree length (Schuh 2000). However, the strict consensus of rc based SACW was two steps longer (346 steps) than the strict consensus tree of the original data and than the ci based SACW strict consensus tree (both 344 steps, Fig. 65). The congruence in tree topology was relatively high between both strict consensus trees yielded from SACW differing only in two nodes of ci based SACW strict consensus (Fig. 65, asterisk), which failed into polytomy in rc based SACW strict consensus.

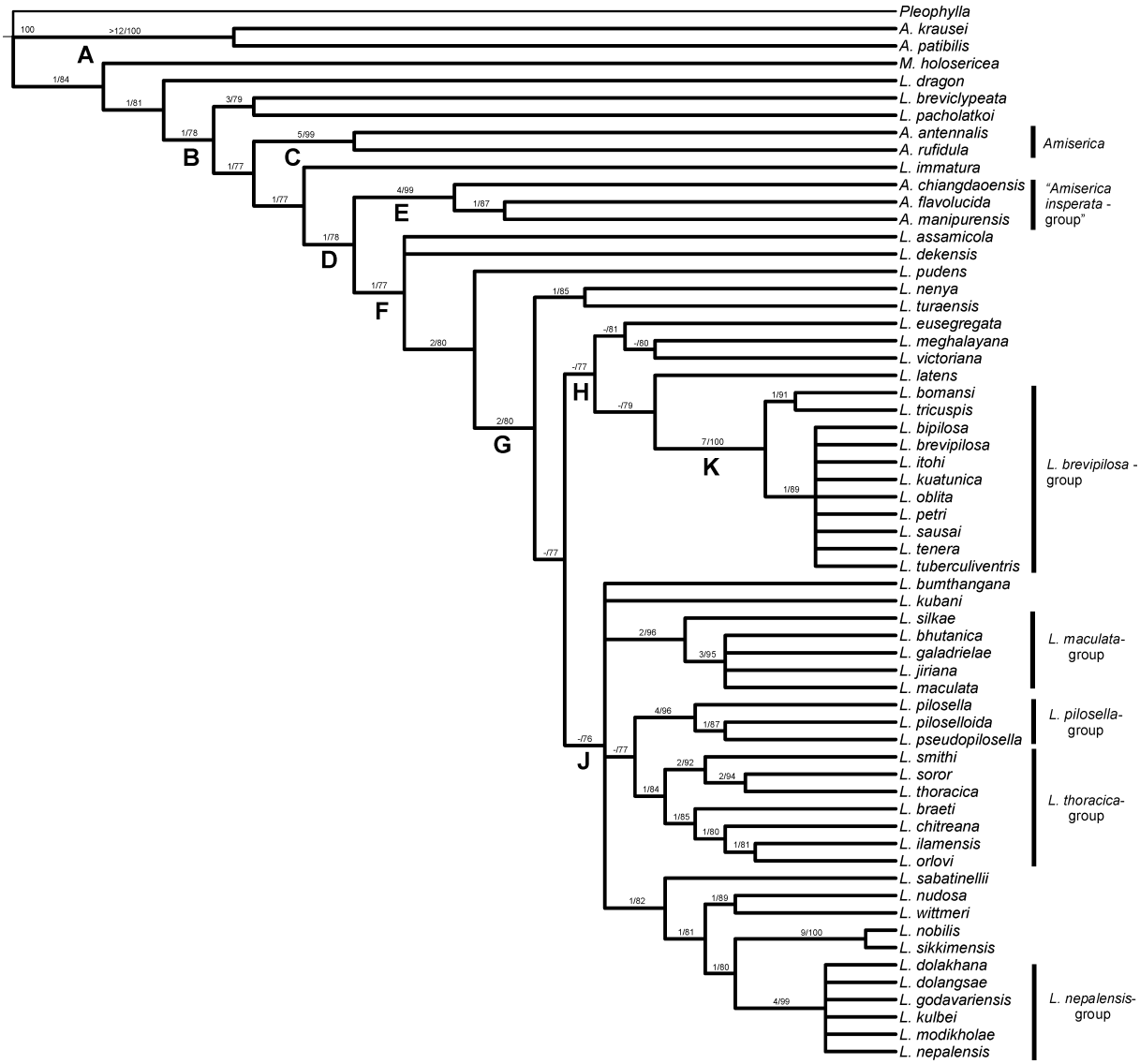


**Fig. 63.** Strict consensus (357 steps, CI: 0.36, RI: 0.71) of 356 equally parsimonious trees (344 steps, CI: 0.37, RI: 0.72) resulting from parsimony ratchet based on equally weighted characters; above each branch support indices (Bremer support/ jackknife values) are shown, below some branches selected nodes were named by capital letters (*A.* = *Amiserica*, *L.* = *Lasioserica*, *M.* = *Maladera*).

## Discussion

### *Characters and computer analysis*

Being as long (344 steps) as the MPTs of the parsimony ratchet analysis with unweighted characters, but being shorter than the majority rule tree (347 steps) resulting from MPTs of analysis with unweighted characters, as well as due to highest resolution, the strict consensus (Fig. 65) resulting from successive approximation based on consistency index is considered as the preferred hypothesis resulting from present data set. Based on this tree further character

evolution and evolutionary diversification of *Lasioserica* are discussed. Changes in topology after SACW are due to one set of characters supporting a competing topology being down weighted (e.g. when ri: 0) for their poor performance elsewhere in the tree.


**Fig. 64.** Majority rule consensus (347 steps) of the 330 equally parsimonious trees (344 steps, CI: 0.37, RI: 0.72) resulting from parsimony ratchet based on equally weighted characters; above each branch is given the frequency (%) of a node among all MPTs (*A.* = *Amiserica*, *L.* = *Lasioserica*, *M.* = *Maladera*).

## *Monophyly of Lasioserica and implications on classification*

*Lasioserica* is one of the sericine genera, known to occur in the mountains of South Asian mainland, only. All species occur in forest habitats, from 400 to over 4000 meters, however, without forming high altitude specialists. The taxonomy and distribution of the genus have been revised recently (Ahrens 1996, 1999b, d, 2000, 2004b) exploiting collection material from numerous private collections and public institutions available to the author's study.

The phylogenetic analysis demonstrated that the representatives of the genus *Lasioserica*, those which fit the original diagnosis of Brenske (1896) (char 35:1, node B, Figs 63, 65), are not monophyletic, since within are nested representatives of the genus *Amiserica*. These *Amiserica* taxa comprise not only the representatives of the *Amiserica insperata* - group (node E) as hypothesized here, by its three exemplarily included species, a presumably

monophyletic group including seventeen species which are distributed from eastern Himalaya to northern mountainous parts of Indochina, but also the type species of *Amiserica*, *A. rufidula*, from Taiwan. At the same moment, the taxa so far included in *Amiserica* prove not to be monophyletic, whilst the Taiwanese taxa *Amiserica rufidula* Nomura, 1974 and *Amiserica antennalis* (Nomura, 1974) comb. n. constitute a robustly supported monophyletic clade (node C, Bremer index: 5, jackknife value: 99%).

Consequently, the use of *Amiserica* should be strictly limited (to the type species and its sister, *A. antennalis*. The taxa of the formerly *Amiserica insperata* - group (node E) should not be assigned to *Amiserica*. However, a valid use of the genus name *Amiserica*, would imply under assumption of present phylogenetic hypothesis that at least two taxa (*L. breviclypeata* and *L. pacholatkoi*) must be excluded from *Lasioserica* to avoid paraphyly of *Lasioserica*. Whether a new genus should be established for both species, or whether they should be included with *Lasioserica*, including *Amiserica* too, should be reserved for future studies, in which the systematic position of *Lasioserica* and *Amiserica* within the Sericini is investigated more extensively. The same is valid for the *Amiserica krausei* + *A. patibilis* clade (node A), which is nested basally to *Lasioserica* and according to tree topology is not related either to *Lasioserica* nor *Amiserica*.

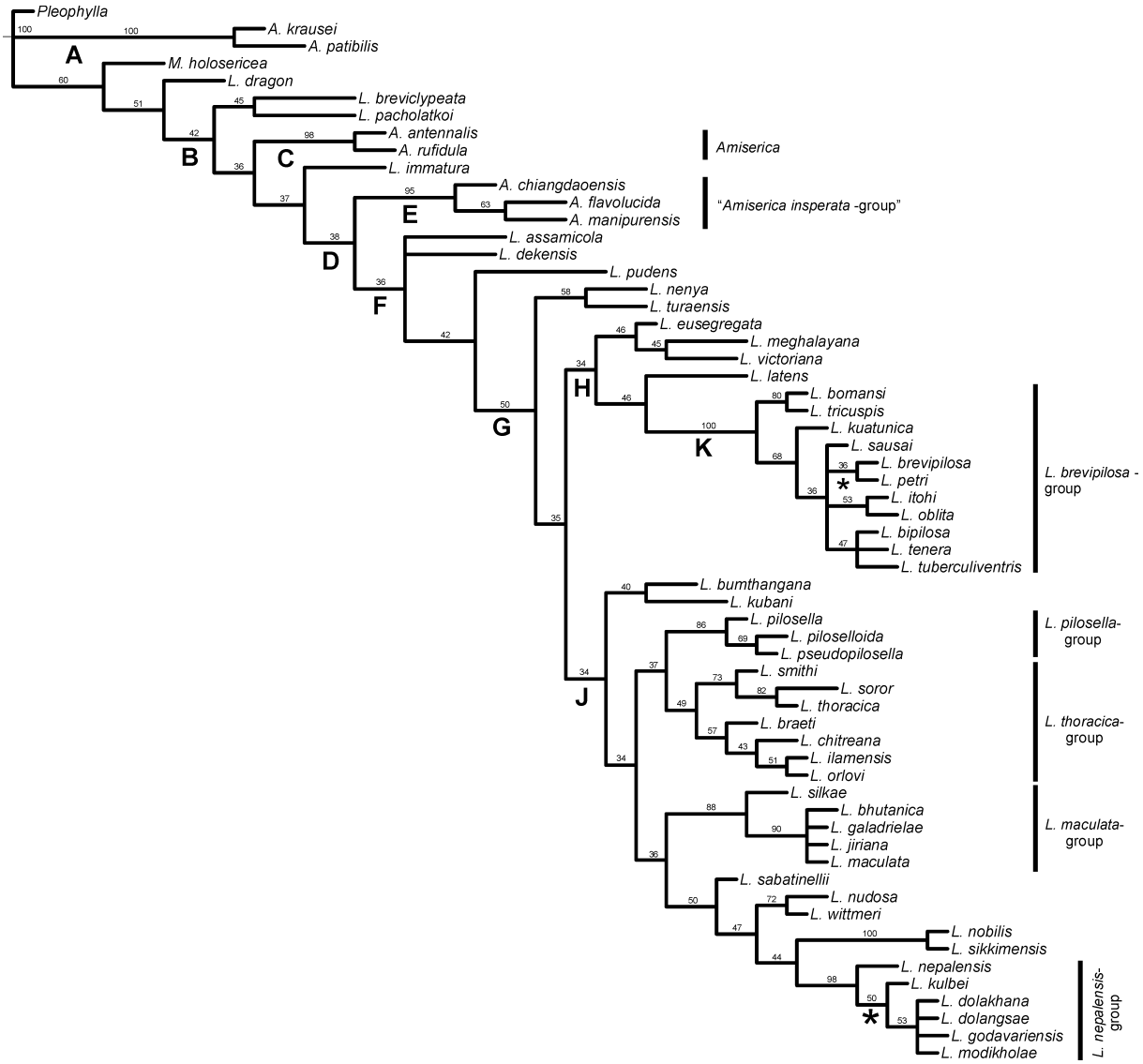


**Fig. 65.** Phylogeny of *Lasioserica*. Strict consensus (344 steps, CI: 0.37, RI: 0.72) tree of 51 equally parsimonious trees (344 steps, CI: 0.37, RI: 0.72) resulting from successive approximation based on consistency index, above each branch support (jackknife) is indicated (*A.* = *Amiserica*, *L.* = *Lasioserica*, *M.* = *Maladera*).

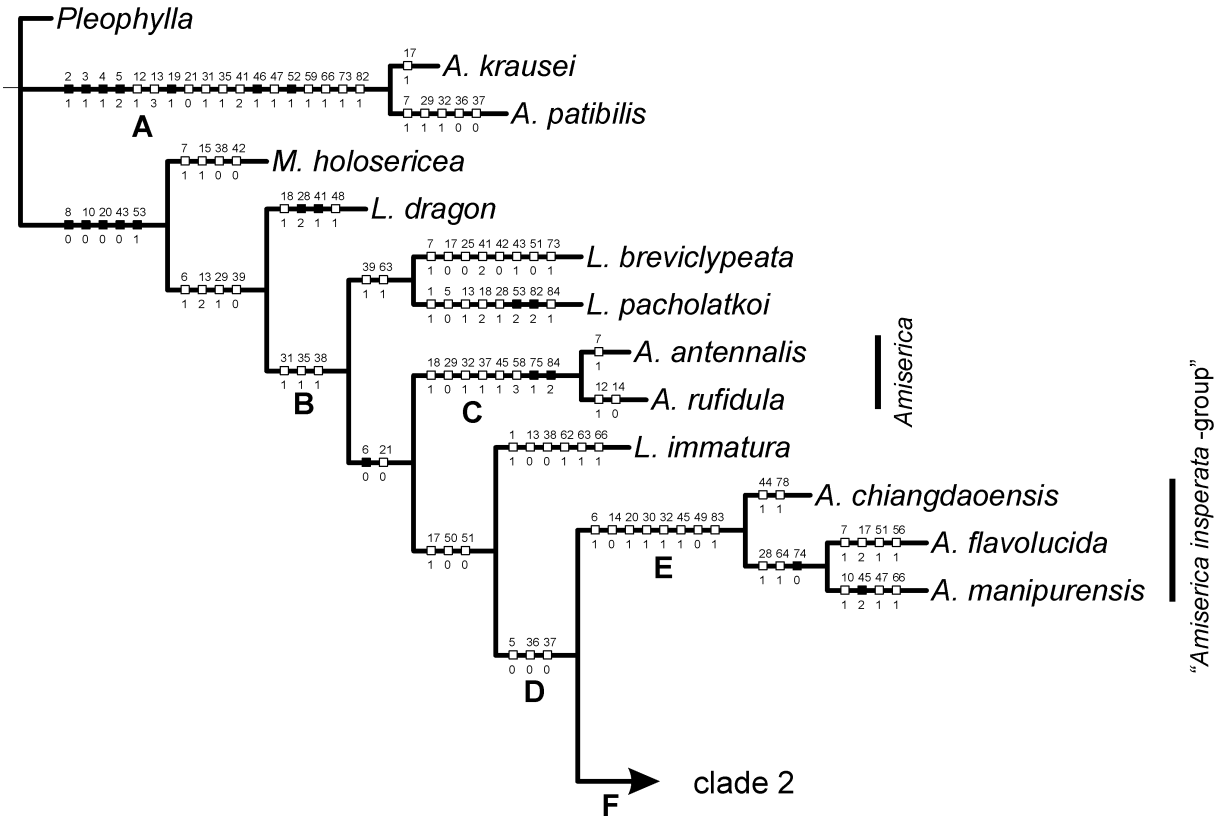


**Fig. 66.** Upper part (clade 1) of strict consensus (344 steps, CI: 0.37, RI: 0.72) tree of 51 equally parsimonious trees (344 steps, CI: 0.37, RI: 0.72) resulting from successive approximation based on consistency index which shows character changes and apomorphies mapped by state (discontinuous characters are mapped as homoplasy and only unambiguous changes are shown, unsupported nodes collapsed and using proportional branch lengths) (full squares: non-homoplasious character states; empty squares: homoplasious character states). Congruent topology in strict consensus tree of both RC based and CI based weighting schemes is indicated by bold branch lines (*A.* = *Amiserica*, *L.* = *Lasioserica*, *M.* = *Maladera*).

The phylogeny yielded from all analyses presented herein showed furthermore that the characters used by Brenske (1896, 1897) to define *Lasioserica* are subject to homoplasy (see 35:1, node A and B). A recently described Chinese species (Miyake and Yamaya 2001) assigned to *Lasioserica*, *L. dragon*, is not nested within the clade at the node B which is supported under 'unambiguous' optimization (Nixon 2002) in total by three apomorphies (Fig. 66): (1) metafemur with submarginal serrated line (31:1, Figs 59C-F), (2) metatibia with longitudinally serrated keel beside dorsal margin (35:1, Figs 59J-O), and (3) apical margin of metatibia on medial face obtusely moderately truncate, producing an indistinct angle with ventral margin (38:1, Fig. 60H). Although *Lasioserica* (taxa sharing node B) + *Lasioserica dragon* in present analysis result to be monophyletic, this hypothesized sister taxon relationship I suppose very likely to fail when additional genera are included which share characters reported by the WINCLADA character changes diagnosis (Fig. 66) as apomorphies for this node, such as the posteriorly dull frons (6:1), the antennal club twice as long as remaining antennomeres combined (13:2), the dorsally serrate posterior margin of metafemur (29:1), and the acutely edged dorsal margin of metatibia (39:0) which under ACCTRAN optimization are completed by further two characters (14:2, 50:1).

Considering the problems of classification of *Lasioserica* generally, the here examined phylogeny for Sericini is a good example of how classification based on phylogenetic systematics is complicated by supraspecific taxa established for endemic lineages based on a (also geographically) limited study of material or for lineages with outstanding autapomorphies making them so "dissimilar from all others". This 'concept' has been widely applied by typologically working taxonomists resulting in the fact, that for example more than 50 % of the genera of Sericini are so far known to be monotypic. Also in the case of

*Lasioserica*, this phenomenon is evident in the establishment of a new genus name, *Orchiserica* Miyake and Yamaya, 2001, for just one species, *Lasioserica brevipilosa* (sic !, see Ahrens 2004b). As a result of the phylogenetic hypothesis on *Lasioserica* elaborated here, the definition of *Lasioserica* and the validity of *Amiserica* as well as the systematic position of *L. dragon* are questionable and need to be revised. This problem, however, I at present consider hardly possible to resolve definitely due to the very limited material available for morphological study. Further, a number of taxa are known just as a few or single specimens, and wide parts of the geographical area under question (e.g. eastern Himalaya, south-eastern Tibetan Plateau, Indochina) are still poorly explored. A solution must be attempted in a wider phylogenetic study of sericine genera.

*Evaluation of clades of Lasioserica*

Based on the original definition of *Lasioserica* (see above), several major clades may be recognized within the genus in its widened sense (including *Amiserica*). A well supported basal clade is that of *L. breviclypeata* + *L. pacholatkoi* whose phallobase is produced apically at right side, with the insertion of parameres protruding (61:1, Figs 62Q,Dd). Their longitudinally serrated keel beside dorsal margin of metatibia is present (35:1, apomorphy for node B) but still more than once interrupted in apical portion (37:2) which should be considered as the plesiomorph character state. In the hypothesized phylogeny they are the sister group to the clade *Amiserica* (in strict sense) + the remainder *Lasioserica* (including the *Amiserica insperata*- group, see Ahrens 2003b). The monophyly of the clade *Amiserica* (in strict sense), *Amiserica rufidula* + *A. antennalis*, is well supported (node C, Bremer support: 5, jackknife value: 99%). Besides a number of homoplasious apomorphies (18:1, 29:0, 32:1, 37:1, 45:1, 58:3, see Fig. 66), they share two important apomorphies not subject to homoplasy: (1) parameres at apex with membraneous sacks (75:1), and (2) temones of endophallus entirely fused mesally (84:2).

While the node of *L. immatura* + remaining taxa of *Lasioserica* (including the *Amiserica insperata*-group) yield low branch support values (Fig. 63), the monophyly of the *Amiserica insperata*-group nested basally within this clade is supported (node E, Bremer support: 4, jackknife value: 99%) by numerous apomorphies (Fig. 66). Among these apomorphies, the absence of the transversely produced antennomere seven (14:0) ( reduction of the number of antennomeres in the antennal club from four to three) is one of the most meaningful since the number of antennomeres in the club has been used as a crucial character in sericine generic systematics and identification since Brenske (1897). The taxa of this clade (node E) included in this analysis are exemplary. The lineage is supposed to comprise a further thirteen species from the Himalaya, Indochina, south-western China and north-eastern India (Fig. 69, Ahrens 2003b).

The node F (Bremer support: 1, jackknife value: 77%) shows an unresolved relationship between *L. assamicola*, *L. dekensis*, and a subsequent clade of *Lasioserica* containing the majority of its presently known extant lineages and species characterized by the following apomorphies: postocular furrow protruding medially towards the interior margin of the eye (9:1), antennal club as long as remaining antennomeres combined (13:0), apical margin of metatibia on medial face weakly and concavely sinuate (it produces with the ventral margin a distinct angle; 38:0), dorsal margin of metatibia moderately carinate (39:1), basal portion temones mesally fused (84:1). This latter clade comprises in addition to its two basal lineages (*L. pudens* and *L. nenya* + *L. turaensis*) two major clades, one mainly diversified in south-western China and northern Indochina (node H), and the second almost confined to the Himalaya (node J).

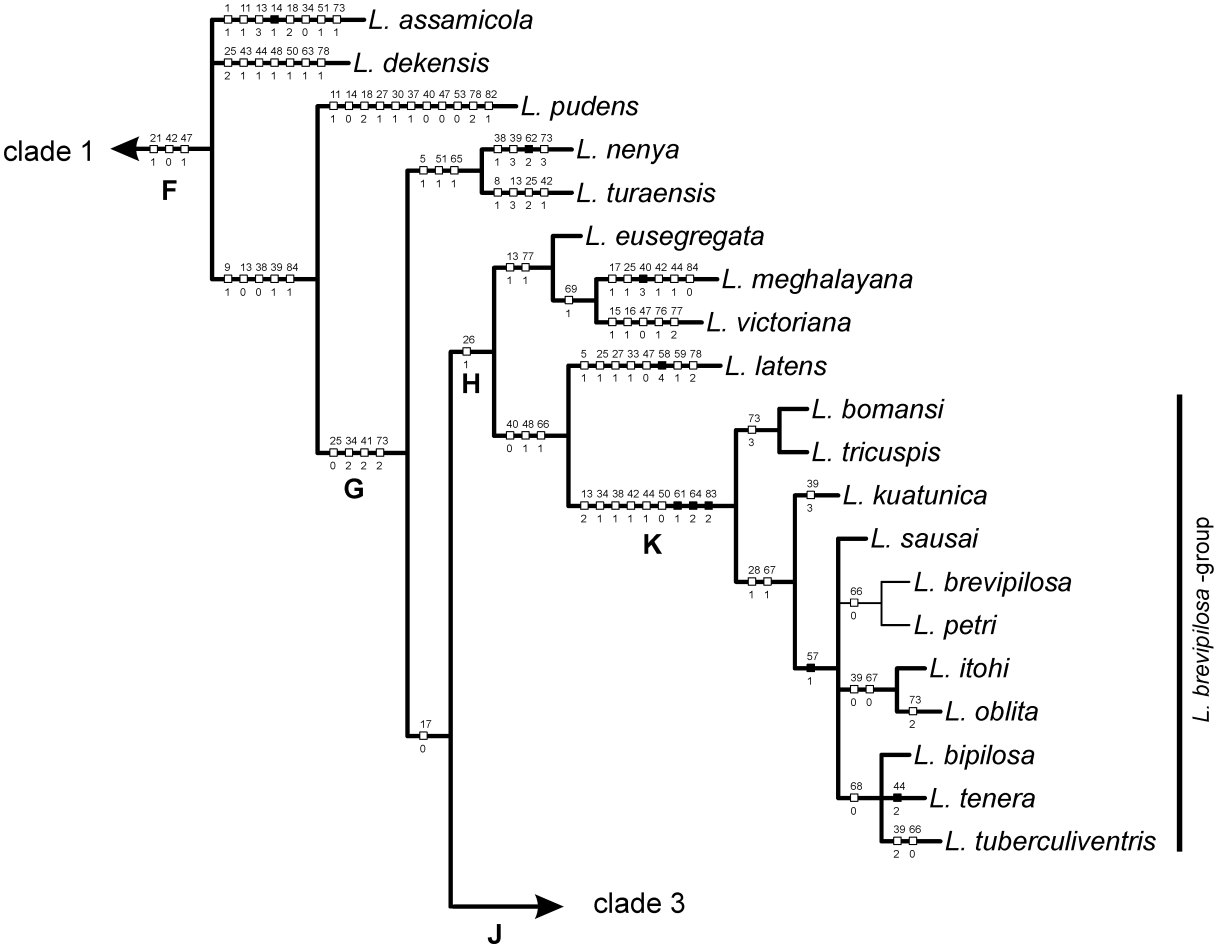


**Fig. 67.** Medium part (clade 2) of strict consensus (344 steps, CI: 0.37, RI: 0.72) tree of 51 equally parsimonious trees (344 steps, CI: 0.37, RI: 0.72) resulting from successive approximation based on consistency index which shows character changes and apomorphies mapped by state (discontinuous characters are mapped as homoplasy and only unambiguous changes are shown, unsupported nodes collapsed and using proportional branch lengths) (full squares: non-homoplasious character states; empty squares: homoplasious character states). Congruent topology in strict consensus tree of both RC based and CI based weighting schemes is indicated by bold branch lines (*L.* = *Lasioserica*).

Within the first lineage we may recognize a clade with highest branch support (node K, Bremer support: 7, jackknife value: 100%), for which I formerly used the name *Lasioserica brevipilosa* – group (Ahrens 2004b). This lineage is most diverse in northern Indochina and Yunnan (China), however, a few taxa occur also further north (*L. tuberculiventris*) and east (*L. kuatunica*) (Fig. 69). They share a relatively large number of apomorphies (Fig. 67), of which those not affected by homoplasy are (1) phallobase mesoapically within sinuation with a triangular median process (61:1), (2) phallobase lateroventrally at apex lamellously produced and elevated (64:2), (3) endophallus with a single dorsal lobe before base of parameres (83:2).

The second principal clade (node J) with lower branch support shows in the strict consensus of the original data set some unresolved polytomies (Fig. 63) which, however, are resolved in the same topology under application of SACW (Fig. 65). Their monophyly is based on two apomorphies: (1) lateral lamina of metafurca anteriorly almost straight and directed ventrally (23:1) and (2) pilosity of metafemur ventrally with a small distance to submarginal serrated line (33:1). Within this clade, in which almost all taxa occur exclusively in the Himalaya, a number of well supported lineages may be outlined. These lineages more or less widely overlap with each other in the Central and eastern Himalaya (Fig. 70) in the cumulative ranges of their included species. Apomorphies supporting each of these nodes are

depicted in Fig. 68. Interestingly, according to present knowledge endemic taxa of this lineage are completely absent in western Himalaya, and only one species (*L. maculata*) extends its range west of the Central Himalaya (Ahrens 2004b).

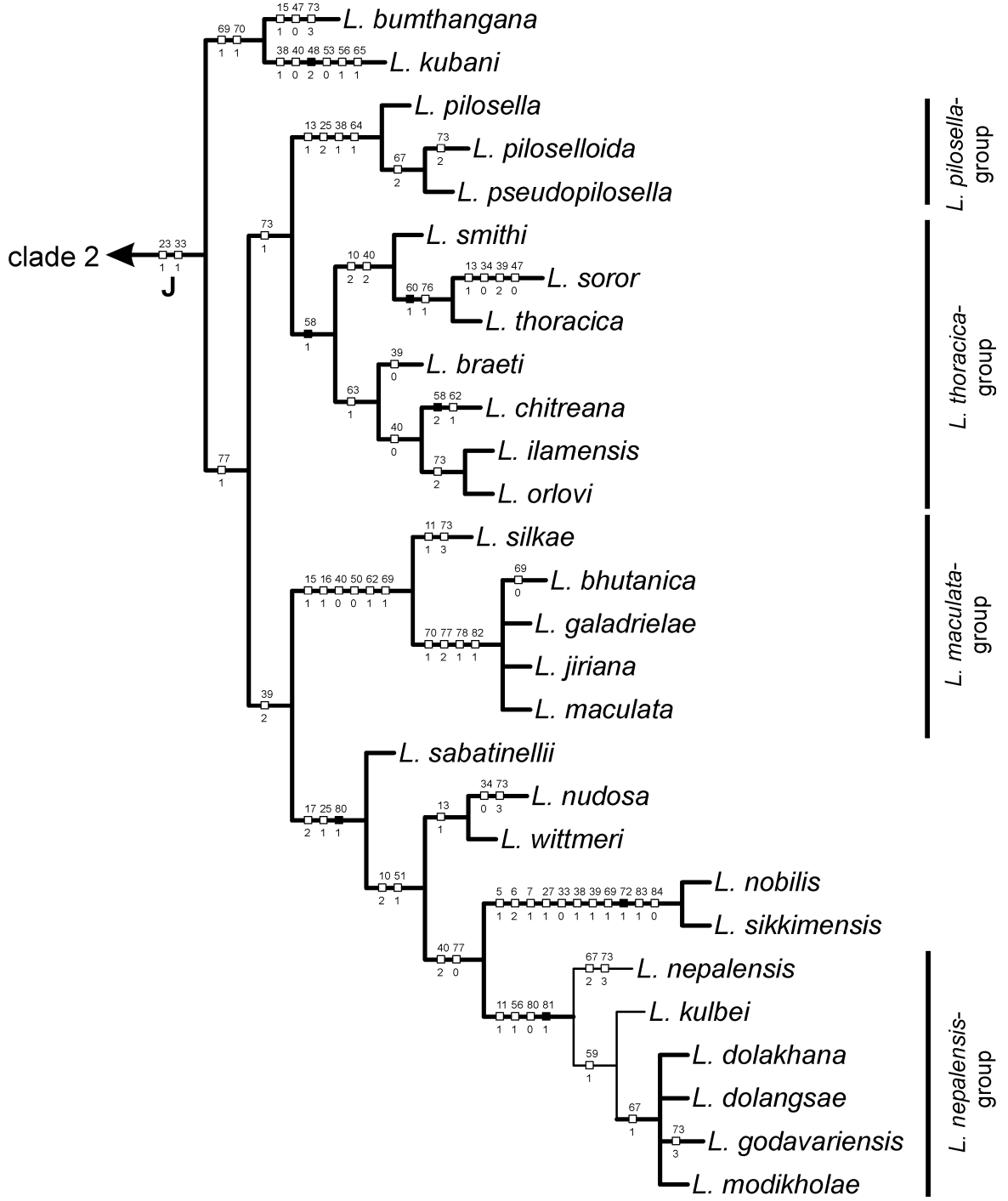


**Fig. 68.** Lower part (clade 3) of strict consensus (344 steps, CI: 0.37, RI: 0.72) tree of 51 equally parsimonious trees (344 steps, CI: 0.37, RI: 0.72) resulting from successive approximation based on consistency index which shows character changes and apomorphies mapped by state (discontinuous characters are mapped as homoplasy and only unambiguous changes are shown, unsupported nodes collapsed and using proportional branch lengths) (full squares: non-homoplasious character states; empty squares: homoplasious character states). Congruent topology in strict consensus tree of both RC based and CI based weighting schemes is indicated by bold branch lines (*L.* = *Lasioserica*).

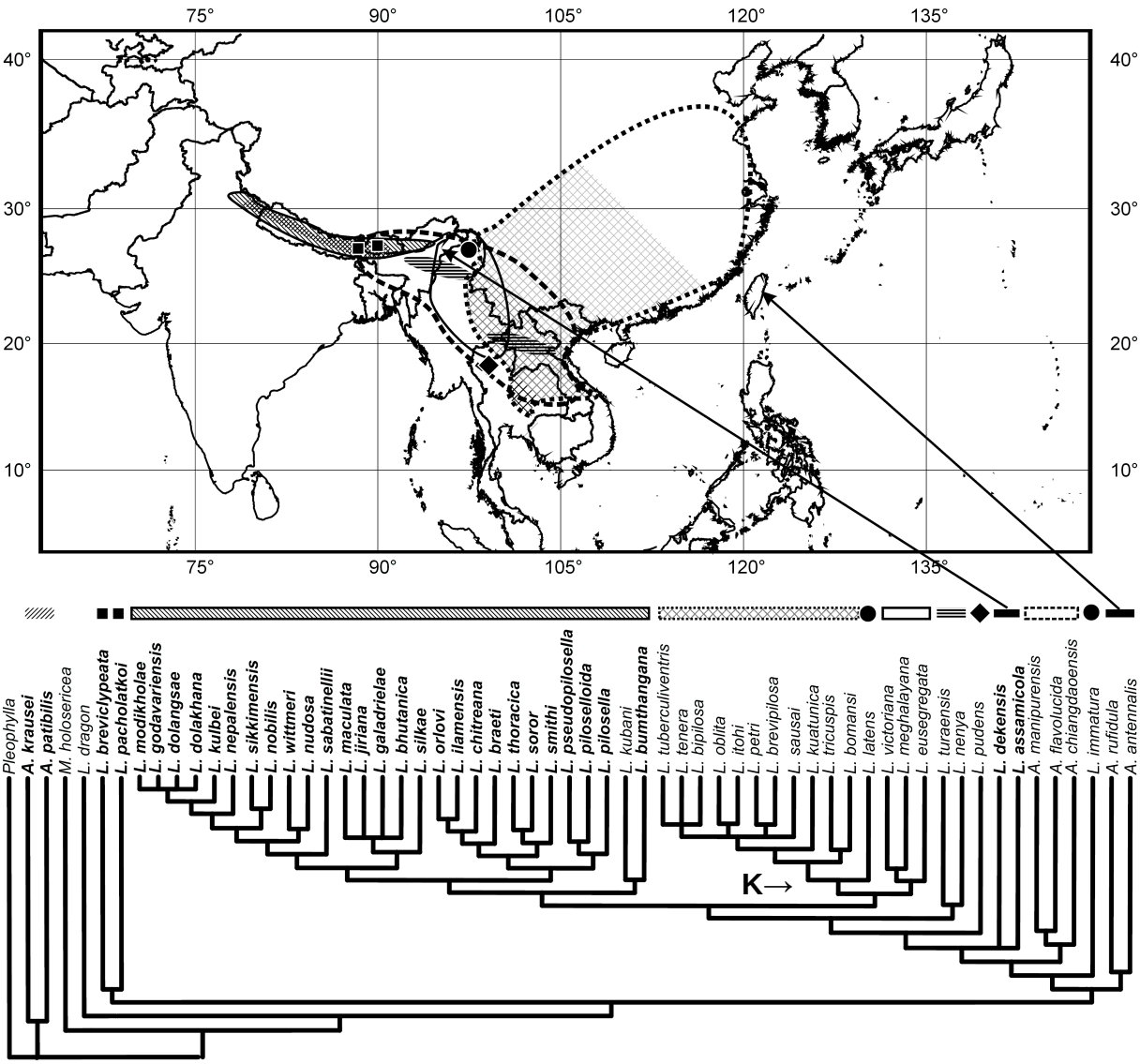


**Fig. 69.** Phylogeny of *Lasioserica* in its geographical framework. Himalayan species are given in the tree in bold letters. The presumptive range of the *L. brevipilosa* clade (see node K), is generally outlined by a dotted line, but from wide parts of it the group is reported by a single species only. Therefore, the core range is marked, additionally, by crossed hatching (*A.* = *Amiserica*, *L.* = *Lasioserica*, *M.* = *Maladera*).

## *Evolution of the genus Lasioserica*

Based on preliminary studies (Ahrens in press) on the phylogeny of Sericini, the species of *Lasioserica* (in its wider sense, node B, Fig. 63) should be nested within the lineage of 'modern Sericini' which share the following apomorphies: the presence of a carina from craniolateral margin of mesosternum to mesofurcal arm, the acutely bent anterior anal vein (AA). A great part of the more than two hundred described sericine genera presumably belong to these 'modern Sericini' absent only in Notogea and Neotropics, but the relationships of these taxa are still completely unexplored.

Due to present distribution pattern of major sericine lineages it must supposed that Sericini have diversified after the break up of Gondwana, probably on the African continent (Ahrens in press), and consequently we should assume neither that the ancestor of *Lasioserica* originated on the Cretaceous Asian continent nor that they arrived in Asia drifting on the Indian continental plate. Based on the present fossil record with first reliable evidence for Sericini from Oligocene (Krell 2000), we may expect for *Lasioserica* and its stem lineage taxa, that they very likely do not predate that period.

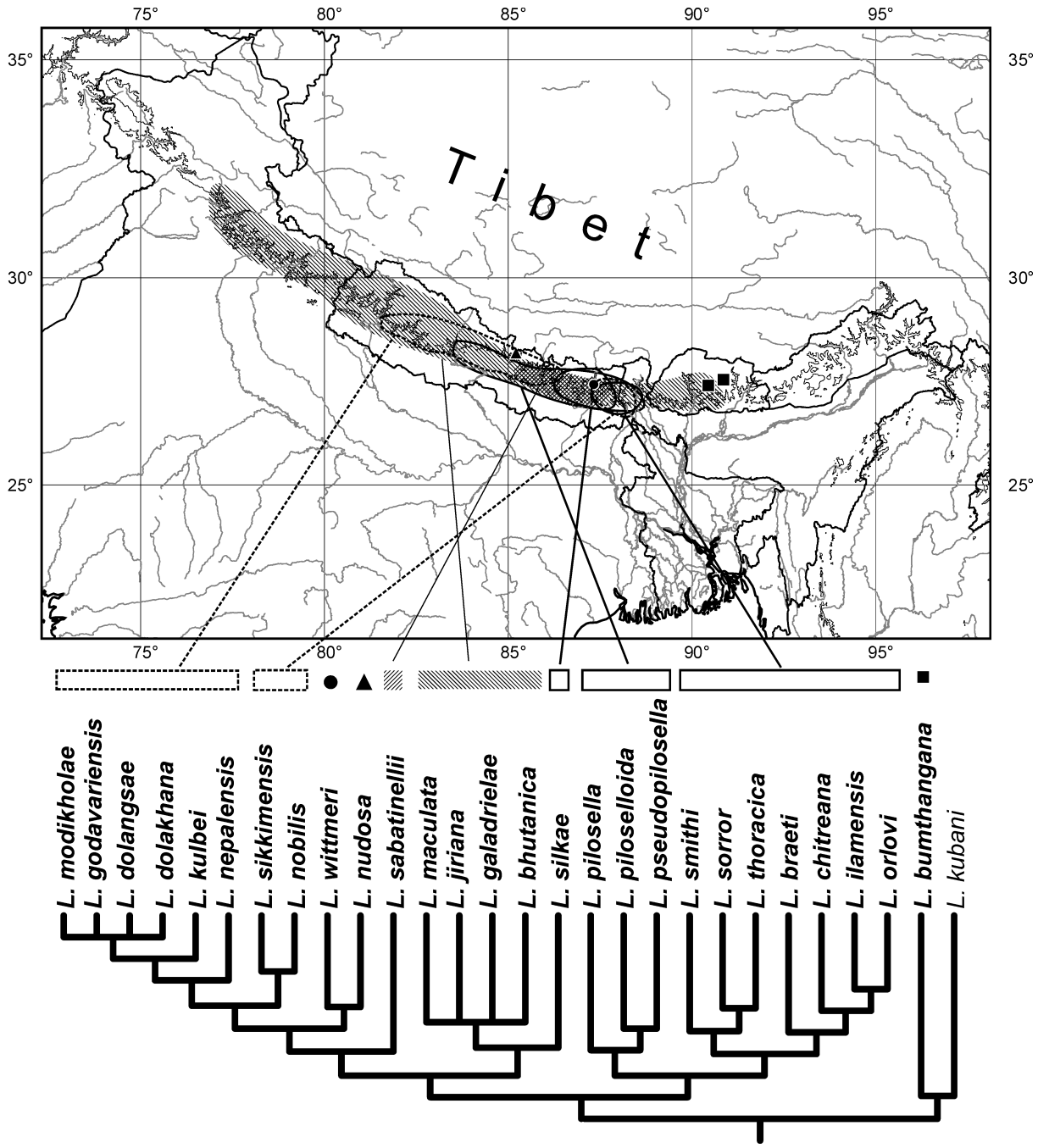


**Fig. 70.** Phylogeny of the almost exclusively Himalayan clade of *Lasioserica* in its geographical framework, Himalayan species are given in the tree in bold letters; *L. kubani*, only, occurs not in the Himalaya (*L.* = *Lasioserica*).

Presently in Himalaya very restrictedly occurring basal lineages of *Lasioserica*, such as *L. pacholatkoi*, *L. breviclypeata*, *L. dekensis*, or *L. assamicola* should be interpreted as relics of former widely distributed clades. Most of the taxa of these clades became extinct, probably partly as consequence of competition of the strongly radiating younger lineages. Other taxa considered exemplarily in the analysis but according to the phylogenetic hypothesis not related to *Lasioserica* performed a radiation similar to the Himalayan *Lasioserica*, such as the clade *Amiserica krausei* + *A. patibilis* which comprises five other species from the Himalaya (Ahrens 2004b).

There is comparatively good evidence from range positions of closely related species for allopatric geographical speciation in *Lasioserica* with the majority of closely related Central-Himalayan species occurring allopatrically or parapatrically, such as the taxa of the

*Lasioserica nepalensis*-group, of the *L. maculata*-group, or of the *L. pilosella*-group (Ahrens 2004b). However, in the more easterly distributed lineages, such as the *L. thoracica*-group, this pattern is reversed, with a great part of closely related species occurring sympatrically, such as *L. soror* + *L. thoracica*, *L. nobilis* + *L. sikkimensis*, *L. orlovi* + *L. ilamensis*. This differentiated pattern might be attributed to the climatic gradient in present and past which has characterized this mountain range at least since the onset of monsoon climate with its humid south-eastern summer winds. The widely expanded westerly range extension of the most western taxa of *Lasioserica*, such as *L. maculata maculata* (Fig. 72) or *L. nepalensis*, in comparison to the rather minute relatively of their closest relatives, is consistent with such a hypothesis.

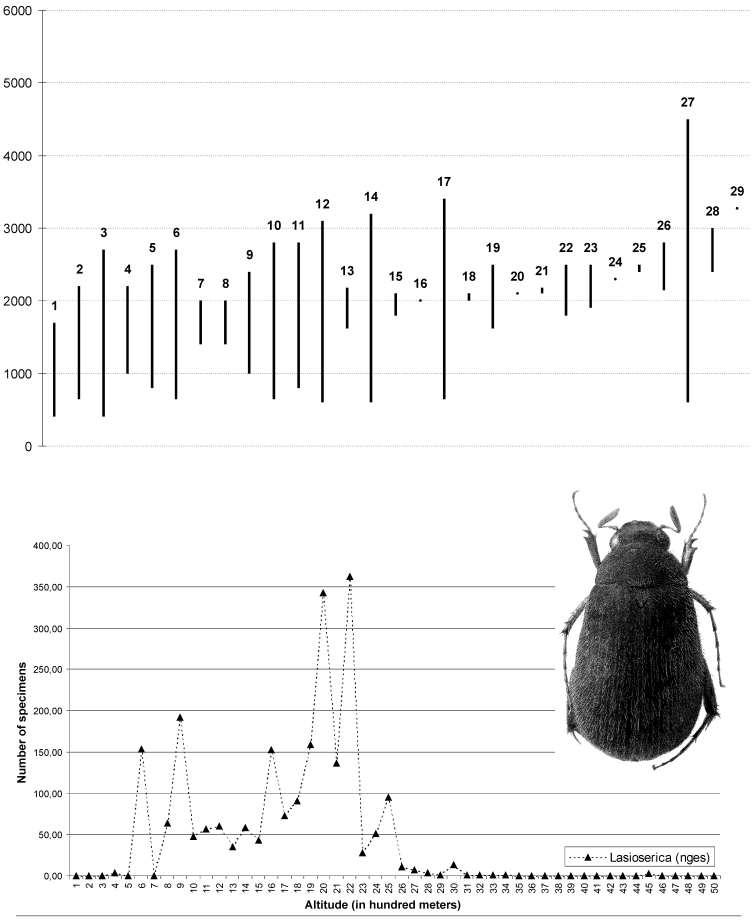


**Fig. 71.** Altitudinal distribution of the Himalayan taxa of *Lasioserica*: 1: *L. dekensis*, 2: *L. maculata galadrielae*, 3: *L. pilosella*, 4: *L. modikholae*, 5: *L. pseudopilosella*, 6: *L. silkae*, 7: *L. godavariensis*, 8: *L. maculata bhutanica*, 9: *L. piloselloida*, 10: *L. chitreana*, 11: *L. kulbei*, 12: *L. maculata maculata*, 13: *L. braeti*, 14: *L. maculata jiriana*, 15: *L. ilamensis*, 16: *L. orlovi*, 17: *L. sabatinellii*, 18: *L. dolakhana*, 19: *L. nobilis*, 20: *L. wittmeri*, 21: *L. soror*, 22: *L. sikkimensis*, 23: *L. thoracica*, 24: *L. dolangsae*, 25: *L. breviclypeata*, 26: *L. bumthangana*, 27: *L. nepalensis*, 28: *L. pacholatkoi*, 29: *L. nudosa* (above). Total number of records in relation to altitude (in hundred meter steps) cumulated from all Himalayan representatives of *Lasioserica* (below).

Additionally, the ecological characteristics of the species of *Lasioserica*, as indicated for example by their altitudinal amplitude, imply that the preferred ecological amplitude is rather restricted from 600 to 2200 meters (Fig. 71), and taxa have not properly diversified along the altitudinal gradient. In fact, this narrow zone of ecological optimum consisting of high humidity combined with relatively elevated temperatures was shown to be affected by aridity since the Pliocene (Igarashi et al. 1988) and especially during the Pleistocene (Chauhan 2003, Vishnu-Mitre and Sharma 1984). Apperently, in western parts of the Himalaya the humid montane belt was more vulnerable to the influence of climatic change. Conclusions of this kind are supported by the results of Yonebayashi and Minaki (1997) demonstrating only little vegetational change from Pleistocene to Holocene in eastern Nepal which are contrasted for example by Pleistocene loess accumulation in the north-western parts of the Himalaya (e.g. Rendell et al. 1989).

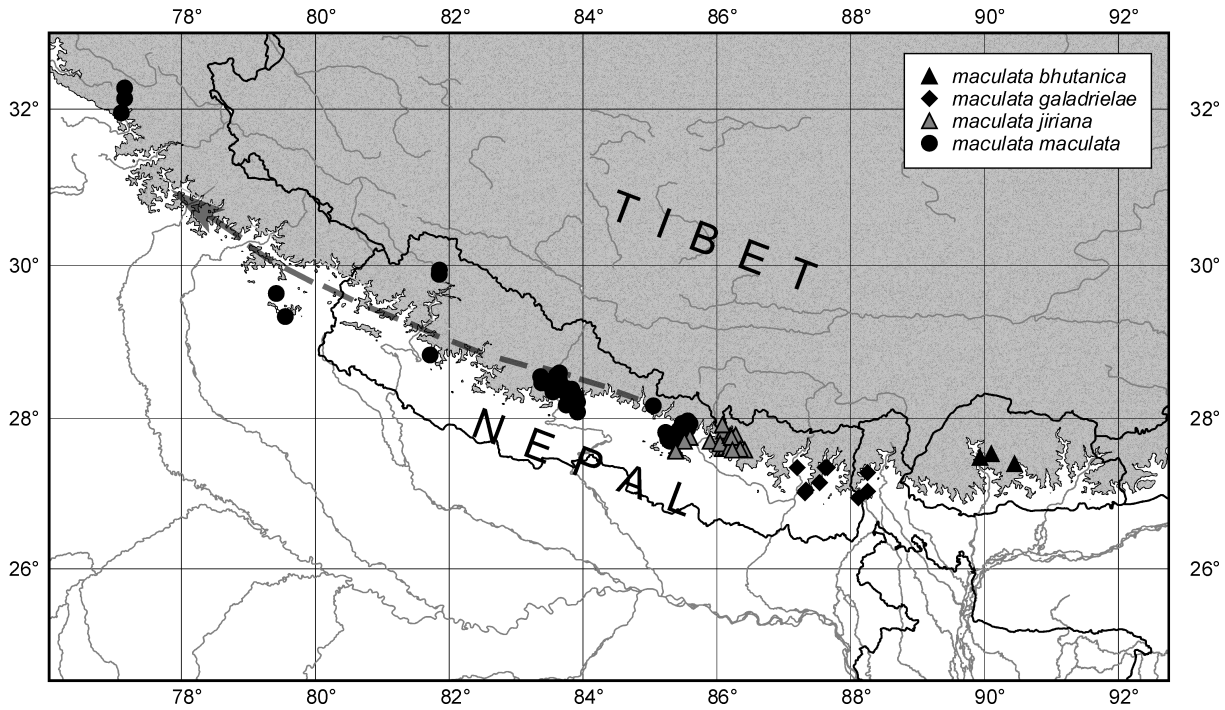


**Fig. 72.** Westerly range extension (indicated by the grey arrow with discontinuous line) of *Lasioserica maculata maculata* in comparison to the other subspecies of *L. maculata* (areas above 2000 meters are grey shaded).

In all respects, diversification of the almost strictly Himalayan clade of *Lasioserica* should not be attributed to a recent occupation of the Himalaya from adjoining areas but to a rather long and persistent evolution in the Himalaya. This would be consistent with the overlapping cumulative ranges of the major lineages of the Himalayan clade as outlined in Fig. 70. This hypothesis finds geological support in new tectonic models predicting high ages for the Himalaya and the southern Tibetan plateau. The rise of the high Tibetan plateau probably occurred in three main steps, by successive growth and uplift of 300- to 500-kilometer-wide crustal thrust-wedges (Tapponier et al. 2001) since the Eocene.

The opportunities for a faunal exchange between the Himalaya with other regions must have been rather limited, since only few species or lineages appear to have dispersed from Himalaya to Indochina (*L. kubani*) or vice versa (*Amiserica sparsesetosa* belonging to the *A. insperata*- group) suggesting a strong 'filter effect' of lowlands (Assam) between the Asian mountain ranges and/or narrow suitable habitat along mountain ranges of the eastern Himalaya.

While Himalayan *Lasioserica* is dominated by one major lineage, those occurring in northern Indochina are much more numerous (Fig. 69). These mountainous areas show a rather similar climate to those of the Central and eastern Himalaya. Interestingly, Songtham et al. (2003) reported from basins in northern Thailand close to these zones a shift from temperate to tropical plant assemblages from Oligocene to Miocene which the authors attribute to the south-eastward extrusion of the Southeast Asian Landmass with its simultaneous clockwise rotation (Tapponier et al. 1986). This process was accompanied by folding and plateau building in the area of the present Shan-Thai Plateau since Eocene (Tapponier et al. 2001).

Apparently, the fact that the species of *Lasioserica* prefer the warm temperate and humid climate of lower montane zone might be an explanation why *Lasioserica* neither diversified in the parts of north-eastern Tibetan Plateau including the ranges of Sichuan and Shaanxi to a great extent nor expanded to the Japanese islands. Accordingly, *Lasioserica* do not shape that typical Sino - Japanese distribution range known for many organisms of the montane zone in the Himalaya (Dobremez 1976). However, how can one explain the obvious scarcity of

endemic species or lineages in south-eastern China and Yunnan ? A hint for further implications might be the absence of modern lineages of *Lasioserica* in Taiwan although this Island was connected with the Asiatic Landmass during the Pleistocene, which could indicate that eastern China was occupied relatively late by representatives of the *L. brevipilosa*- group, when the land bridge was re-interrupted after the Pleistocene by rising sea level. In fact, Zheng et al. (1998) reported that temperate deciduous forests in eastern China were replaced by boreal conifers during Last Glacial Maximum (at ca. 8 ka) which indicates a colder climate and less favourable conditions in these regions for warm temperate taxa, such as the species of *Lasioserica*.

The results presented here, although beginning to reveal an overall phylogenetic framework for *Lasioserica* that is relatively robust, as well as suggesting a number of well supported species relationships, are still very far from satisfactory. Within all Sericini examined in the course of these studies, the extreme homogeneity in adult morphology left many of deeper nodes especially those indicative of basal lineages or generic relationships, unresolved or poorly supported. For many taxa, sometimes only the holotype or a small number of specimens were available for examination, often known only in one sex. Being still completely unexplored faunisticly, we have to expect still numerous new species from the eastern Himalaya, in particular in the ranges of Arunachal Pradesh, which surely would contribute significantly to our more comprehensive understanding of the climate – biodiversity interactions in this region.